Electrochemical and structural properties of V_2O_5 thin films prepared by DC sputtering

C. Navone[a], J.P. Pereira-Ramos[a,*], R. Baddour-Hadjean[b], R. Salot[c]

[a] *Institut des Sciences Chimiques Seine Amont, LECSO, UMR CNRS 7582, CNRS 2 rue Henri Dunant 94320 Thiais, France*
[b] *Institut des Sciences Chimiques Seine Amont, LADIR, UMR CNRS 7075, CNRS 2 rue Henri Dunant 94320 Thiais, France*
[c] *CEA Grenoble, CEREM-DEM, 17 rue des Martyrs 38054 Grenoble, France*

Abstract

Vanadium pentoxide thin films have been prepared by reactive DC magnetron sputtering from a vanadium metal target without annealing posttreatment. XRD, Raman and electrochemical experiments on 800 nm thin films show a high crystallinity of the deposits. Chronopotentiometric measurements performed in the two voltage range 3.8–2.8 and 3.8–2.15 V have demonstrated the promoting effect of the $h\,0\,0$ preferred orientation of V_2O_5 films in terms of polarization, kinetics and rate capability. The same reproducible deposition method is successfully applied to get films thicker than 1 μm in order to optimize the specific capacity. Effective high specific capacities can be then obtained with films 2.4 μm thick tested at high constant current density (100 μA cm^{-2}): a stable capacity of 75 μAh cm^{-2} is available over 100 cycles in the 3.8–2.8 V potential range and 130 μAh cm^{-2} are still recovered in the range 3.8–2.15 V. These results indicate a promising cycling behaviour can be expected with thick films exhibiting a preferred orientation corresponding to V_2O_5 planes perpendicular to the substrate.
© 2005 Elsevier B.V. All rights reserved.

Keywords: Vanadium pentoxide; DC magnetron sputtering; Thin film; Lithium batteries

1. Introduction

Recently, attention has been focused on the research and development of microbatteries owing to the growing miniaturization of electronic devices. The reduction of the current and the power requirements of the electronic devices has resulted in the development of thin-film materials. The energy storage capacity of the thin-film battery is mainly dependent on the cathode material used. Among various kinds of transition metal oxides, V_2O_5 exhibits the most attractive capacity in the potential window 3.8–1.5 V [1–4] and very promising properties have been reported when vanadium oxide thin films are grown by sputtering methods. In the present work, we report the structural and electrochemical characteristics of V_2O_5 films prepared by DC sputtering using a vanadium metal target. In particular, the influence of some deposition parameters such as the oxygen flow ratio and DC power on the morphology of the film oxides is investigated.

2. Experimental

Vanadium oxides films were deposited in a Plassys IMD 700 apparatus on a nickel substrate (10 μm thick Ni foils) by DC magnetron reactive sputtering using a vanadium metal target (99.7%) of 100 mm diameter. The target to substrate distance was 130 mm. Before deposition, the substrates were first cleaned in an ultrasonic bath with acetone and ethanol and then exposed to an Ar/H_2 atmosphere for 15 min to ensure a complete cleaning of the surface. The films growth was performed in an Ar/O_2 atmosphere with a constant argon flow of 46 sccm (partial pressure of 0.5 Pa) and a variable oxygen flow rate. Two DC powers were used, 500 and 1000 W. The film thickness was controlled by deposition time and measured by a profilometer. The surface morphology of the deposited films was investigated by scanning electron

---

microscopy using a LEO 1530SEG apparatus. X-ray diffraction (XRD) data were collected using a Brucker D8 Advance diffractometer with Cu Kα radiation ($\lambda_{K\alpha} = 1.5406\,\text{Å}$). The Raman spectra were recorded using a Labram spectrometer including a charge coupled device (CCD) detector. A Nd:YAG laser generating a green beam at the wavelength 532 nm was used as the excitation source.

Electrochemical studies were carried out in two-electrodes cells (Swagelok® type) using $1\,\text{mol}\,\text{L}^{-1}$ $LiClO_4$ in propylene carbonate as electrolyte. The cell was prepared inside a dry box by placing a clean lithium metal disk (12 mm diameter), a glass fiber separator soaked with the electrolyte solution and the cathode film ($0.5\,\text{cm}^2$) into a Teflon container with two stainless steel terminals. Galvanostatic and voltammetric measurements were made with a 1470A Solartron controlled by a computer. The current densities applied are in the range 1–$100\,\mu\text{A}\,\text{cm}^{-2}$.

Impedance measurements were made, in the frequency range 4×10^4 to $4 \times 10^{-3}\,\text{Hz}$, with an E.G.G. 273A apparatus connected with an E.G.G. 5208 Two Phase Lock-in Analyser drived by an IBM computer. The excitation signal was 10 mV peak to peak. The equilibrium potential was considered to be reached when the drift in open circuit voltage remained less than 0.2 mV for 1 h.

3. Results and discussion

The experimental sputtering conditions for the deposition of four vanadium oxide films are summarized in Table 1. The thickness of all samples was 800 nm except for sample A, 550 nm thick. The V_2O_5 active mass was determined by weighing experiments and by analysis for vanadium content (atomic absorption spectrometry) after dissolution of the deposit in $0.5\,\text{M}\,H_2SO_4$.

Fig. 1 shows XRD diffraction patterns of vanadium oxide films as obtained. Depending on the sample, seven diffraction lines corresponding to the orthorhombic V_2O_5 phase (space group *Pmmn*) appear, the 200, 001, 101, 110, 400, 002 and 600 diffraction peaks [JCPDS 41-1426]. The lattice parameters calculated from Fig. 1 for the orthorhombic cell of vanadium pentoxide are very close to that of the polycrystalline oxide powder: $a = 11.50\,\text{Å}$, $b = 3.57\,\text{Å}$, $c = 4.43\,\text{Å}$. The unusual large value of the interlayer parameter c has to be outlined.

Whatever the oxygen flow, the use of a DC power of 1000 W leads to the formation of well crystallized V_2O_5 films
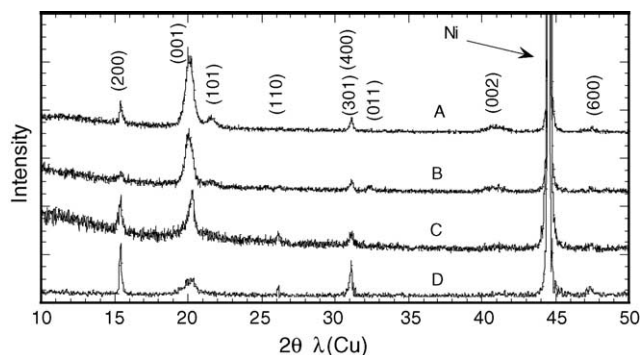

Fig. 1. XRD patterns of 800 nm V_2O_5 thin films deposited on Ni foil by DC sputtering (DC power = 1000 W for samples A and B, and 500 W for samples C and D).

strongly oriented with the *ab* planes parallel to the substrate showing a 001 preferred orientation (samples A and B). Conversely, in samples C and D, the crystallites of V_2O_5 films preferentially grow with a direction and the *ab* planes perpendicular to the substrate indicating a $h00$ preferred orientation. Fig. 2 shows the Raman spectra of pure V_2O_5 film with 001 (sample B) and $h00$ (sample C) orientations. Both spectra exhibit well resolved Raman lines, which is indicative of the high degree of crystallinity of the films. The frequencies of the nine Raman bands observed in the 100–$1000\,\text{cm}^{-1}$ frequency range correspond to those expected for polycrystalline V_2O_5.

Depending on the oxygen flow ratio O_2/Ar, the power used and the substrate, the trends in a specific orientation of V_2O_5 films strongly differ with deposition conditions. Using rf sputtering and an O_2 partial flow rate of 5%, V_2O_5 films have been obtained on ITO substrates also with a $h00$ preferred orientation but only for very thin films which do not exceed 150 nm [5]. Crystallized vanadium pentoxide thin films prepared by sputtering with a $h00$ preferred orientation as thick as 800 nm have never been proposed as lithium intercalation compounds as yet. Indeed previous attempts to
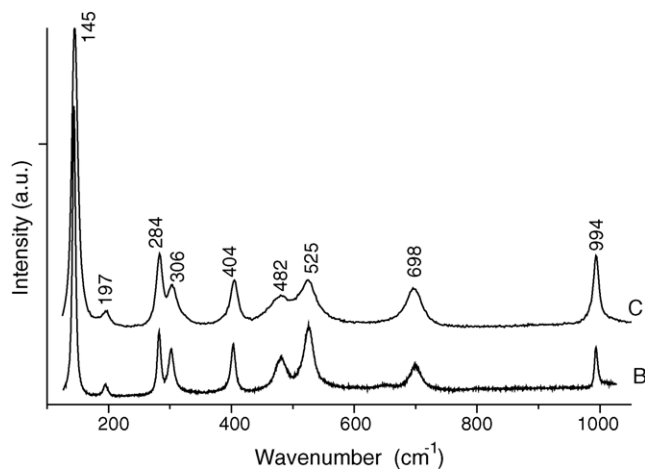
Table 1
experimental conditions for V_2O_5 deposition by DC sputtering

Sample	DC power (W)	O_2 flow rate (sccm)	O_2 partial pressure (Pa)
A	1000	40	0.16
B	1000	80	0.45
C	500	40	0.28
D	500	80	0.50

Fig. 2. Raman spectra of 800 nm V_2O_5 thin films (samples B and C).
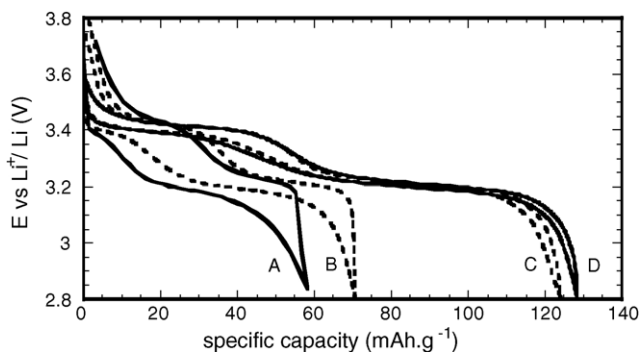
Fig. 3. Discharge–charge curves of V_2O_5 thin films at $10\,\mu A\,cm^{-2}$ (samples A–D).

Fig. 4. Influence of the current density on the first discharge capacity of 800 nm V_2O_5 thin films characterized by a $h\,0\,0$ ($\bigcirc$, sample C) and a $0\,0\,1$ ($\bullet$, sample B) preferred orientation (3.8–2.8 V).

prepare a crystallized 800 nm thick film using rf sputtering led to a mixture of V_2O_5 and V_6O_{13} [6], while thicker films were characterized by a $1\,1\,0$ preferred orientation but poor electrochemical features. Most of works in this area mainly indicate a $0\,0\,1$ preferred orientation for V_2O_5 thin films [4,7].

SEM micrographs confirm samples A and B consist in a stacking of more or less long platelets all arranged parallel to the substrate, i.e. as relatively dense deposits. Samples C and D are viewed as standing platelets perpendicular to the surface of the substrate in good accord with XRD data presented above. This morphology induces a high porosity.

Fig. 3 summarizes the first discharge–charge cycle at $10\,\mu A\,cm^{-2}$ for the four samples in the 3.8–2.8 V voltage range. For samples C and D characterized by a $h\,0\,0$ preferred orientation, the stepwise discharge–charge curve with the two well-defined voltage plateaux located at 3.4 and 3.2 V is found, as expected in the case of the discharge profile for a composite electrode made of polycrystalline V_2O_5 powder [8]. The efficiency of the charge process is 100% and the working potential during reduction and oxidation practically superimpose showing the reversibility of the Li insertion reaction into V_2O_5 thin films. The discharge capacity corresponds to $26\,\mu Ah\,cm^{-2}$, which compares very well with values reported for amorphous thin films in the same voltage range [9]. Taking the deposit mass found for these samples ($\sim 200\,\mu g\,cm^{-2}$) into account, it comes out around 0.9 lithium ions per mole of oxide are intercalated. For more dense deposits, (samples A and B with a $0\,0\,1$ preferred orientation), the two redox steps near 3.4 and 3.2 V are shortened and the capacity is much lower. More information is provided when the influence of the current density on the discharge capacity is investigated for the two kinds of deposits with the same thickness (Fig. 4). Indeed, the $0\,0\,1$ deposits are very sensitive to the current density as shown in Fig. 4.

Except at low rates, the capacity exhibited by the $h\,0\,0$ deposit is significantly larger than that of the $0\,0\,1$ deposit, at least by 30% at 20 and $40\,\mu A\,cm^{-2}$.

It comes out that the $h\,0\,0$ oriented V_2O_5 films probably promotes the kinetics of the electrochemical lithium insertion reaction. This can be explained by an optimization of the electroactive surface area because most of the oxide particles
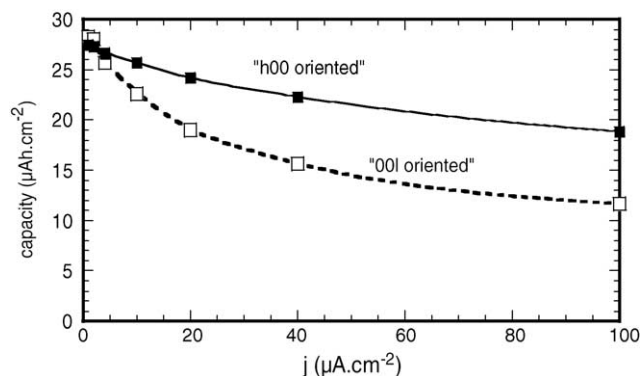
arranged perpendicular to the substrate enhance the porosity of the deposit and then allow an efficient contact between the active material and electrolyte.

A typical ac impedance diagram of a two electrodes cell working with sample C with the composition $Li_{0.26}V_2O_5$ is shown in Fig. 5. In addition to the two semi-circles ascribed to the charge transfer for lithium and the thin-film oxide, a Warburg's region (straight line at 45°) is observed (0.16–0.016 Hz) which is relative to the semi-infinite diffusion phenomenon. At low frequencies, the phase angle increases and the quasi vertical line obtained corresponds to the finite diffusion process. From the relationship Re $Z = f(\omega^{-1/2})$ drawn from the Warburg 'region', the Warburg prefactor is calculated which allows to determine an apparent diffusion coefficient for lithium ions, D_{Li}^{app} of $4 \times 10^{-10}\,cm^2\,s^{-1}$. This high value is consistent with the high rate capability reported above.
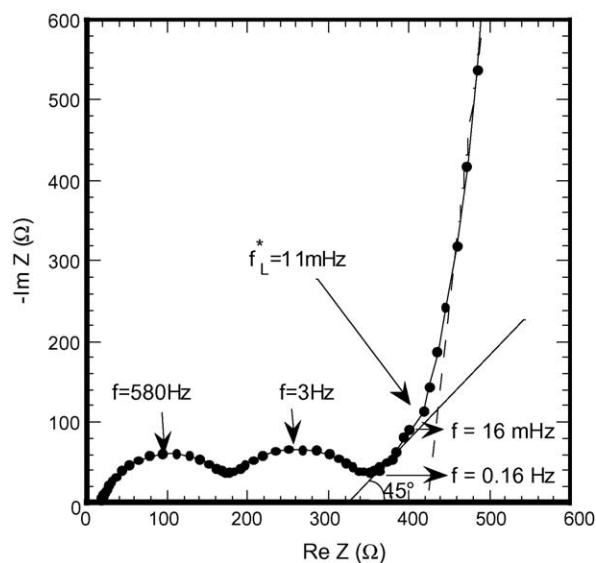

Fig. 5. AC impedance diagram for a 800 nm $Li_{0.26}V_2O_5$ thin film/1 M $LiClO_4$ in PC/Li cell. (V_2O_5 film = sample C).
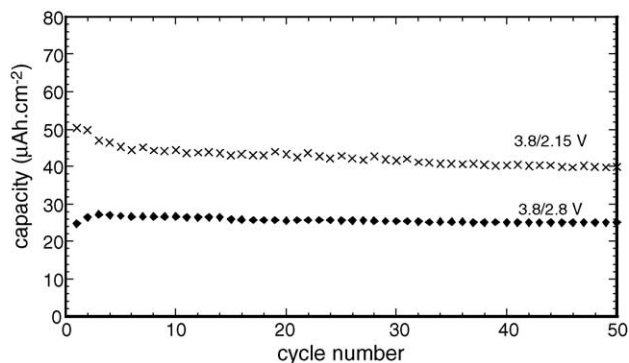
Fig. 6. Evolution of the specific capacity as a function of cycles number for 800 nm V_2O_5 thin film at $10\,\mu A\,cm^{-2}$.

With the aim at improving the specific capacity available with such $h\,0\,0$ oriented thin films, discharge–charge cycling experiments have been performed as a function of the depth of discharge and of the thickness of the deposit. Therefore, films with thickness of 2.4 μm have been successfully synthesized. Figs. 6 and 7 display the cycling properties of V_2O_5 films 800 nm and 2.4 μm thick tested at 10 and $100\,\mu A\,cm^{-2}$, respectively. Two sets of data are observed depending on the potential range. When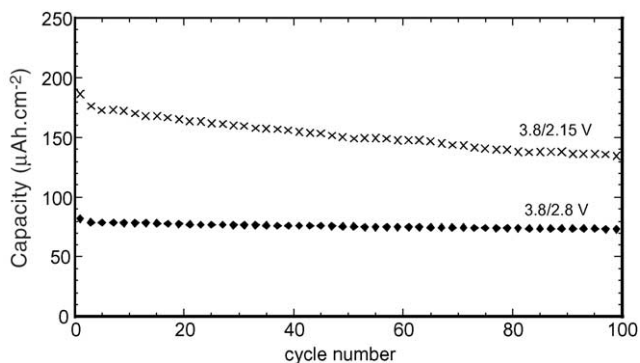 the first two insertion steps are involved in the range 3.8–2.8 V, the capacities are very stable over at least 50 cycles with $22\,\mu Ah\,cm^{-2}$ for the 800 nm thick film and $75\,\mu Ah\,cm^{-2}$ over 100 cycles for the 2.4 μm V_2O_5 film. In the voltage range 3.8–2.15 V, the sample with thickness of 800 nm exhibits a stable capacity of $40\,\mu Ah\,cm^{-2}$ (Fig. 6) after an initial capacity loss, which has not been elucidated. Attractive properties are obtained for the thicker film (Fig. 7) with $130\,\mu Ah\,cm^{-2}$ available after 100 cycles at $100\,\mu Ah\,cm^{-2}$ (C rate). In that case the mid-discharge voltage is 2.8 V. These results compare very well with the best one reported on crystalline and amorphous but thinner V_2O_5 film [3,6,10]. In fact, the specific capacity achieved, with the 2.4 μm thick film constitutes a real improvement insofar as films with thickness over 1 μm are known to display poor cycling properties due to the instability of interface between film and substrate.

Further work is in progress in order to improve the stability of the specific capacity in the potential range 3.8–2.15 V.

Fig. 7. Evolution of the specific capacity as a function of cycles number for a V_2O_5 film 2.4 μm thick at $100\,\mu A\,cm^{-2}$ (C rate).

References

[1] J.B. Bates, N.J. Dudney, D.C. Lubben, G.R. Gruzalski, B.S. Kwak, X. Yu, R.A. Zuhr, J. Power Sources 54 (1995) 58.
[2] J.G. Zhang, J.M. McGraw, J. Turner, D. Ginley, J. Electrochem. Soc. 144 (1997) 1630.
[3] Y.J. Park, K.S. Ryu, K.M. Kim, N.G. Park, M.G. Kang, S.H. Chang, Solid State Ionics 154 (2002) 229.
[4] N. Kumagai, H. Kitamoto, M. Baba, S. Durand-Vidal, D. Devilliers, H. Groult, J. Appl. Electrochem. 28 (1998) 41.
[5] H. Miyazaki, H. Sakamura, M. Kamei, I. Yasui, Solid State Ionics 122 (1999) 223.
[6] Y.J. Park, K.S. Ryu, N.G. Park, Y.S. Hong, S.H. Chang, J. Electrochem. Soc. 149 (2002) 597.
[7] S. Koike, T. Fujieda, T. Sakai, S. Higuchi, J. Power Sources 81–82 (1999) 581.
[8] C. Delmas, H. Cognac-Auradou, J.M. Cocciantelli, M. Ménétrier, J.P. Doumerc, Solid State Ionics 69 (1994) 257.
[9] J.B. Bates, N.J. Dudney, G.R. Gruzalski, A. Zuhr, A. Choudhury, C.F. Luck, J.D. Robertson, J. Power Sources 43–44 (1993) 103.
[10] S.H. Lee, H.M. Cheong, P. Liu, E. Tracy, J.R. Pitts, S.K. Deb, Solid State Ionics 165 (2003) 81.